PHILOSOPHICAL TRANSACTIONS OF THE ROYAL SOCIETY B BIOLOGICAL SCIENCES

Water Vapour, CO<latex>$_{2}$</latex> and Insolation over the Last Glacial-Interglacial Cycles

A. Berger, C. Tricot, H. Gallee and M. F. Loutre

Phil. Trans. R. Soc. Lond. B 1993 **341**, 253-261
doi: 10.1098/rstb.1993.0110

Water vapour, CO_2 and insolation over the last glacial–interglacial cycles

A. BERGER, C. TRICOT, H. GALLÉE AND M. F. LOUTRE

Université Catholique de Louvain, Institut d'Astronomie et de Géophysique G. Lemaître, 2 Chemin du Cyclotron, B-1348 Louvain-la-Neuve, Belgium

SUMMARY

A two-dimensional model which links the atmosphere, the mixed layer of the ocean, the sea ice, the continents, the ice sheets and their underlying bedrock has been used to test the Milankovitch theory over the last two glacial–interglacial cycles. A series of sensitivity analyses have allowed us to understand better the internal mechanisms which drive the simulated climate system and in particular the feedbacks related to surface albedo and water vapour.

It was found that orbital variations alone can induce, in such a system, feedbacks sufficient to generate the low frequency part of the climatic variations over the last 122 ka. These simulated variations at the astronomical timescale are broadly in agreement with reconstructions of ice-sheet volume and of sea level independently obtained from geological data. Imperfections in the stimulated climate were the insufficient southward extent of the ice sheets and the too small hemispheric cooling at the last glacial maximum. These deficiencies were partly remedied in a further experiment by using the time-dependent atmospheric CO_2 concentration given by the Vostok ice core in addition to the astronomical forcing. In this transient simulation, 70% of the Northern Hemisphere ice volume is related to the astronomical forcing and the related changes in the albedo, the remaining 30% being due to the CO_2 changes. Analysis of the processes involved shows that variations of ablation are more important for the ice-sheet response than are variations of snow precipitation. A key mechanism in the deglaciation after the last glacial maximum appears to be the 'ageing' of snow which significantly decreases its albedo. The other factors which play an important role are ice-sheet altitude, insolation, taiga cover, ice-albedo feedback, ice-sheet configuration ('continentality' and 'desert' effect), isostatic rebound, CO_2 changes and temperature–water vapour feedback.

Numerical experiments have also been carried out with a one-dimensional radiative-convective model in order to quantify the influence of the CO_2 changes and of the water vapour feedback on the climate evolution of the Northern Hemisphere over the last 122 ka. Results of these experiments indicate that 67% of the simulated cooling at the last glacial maximum can be attributed to the astronomical forcing and the subsequent surface albedo increase, the remaining 33% being associated with the reduced CO_2 concentration. Moreover, the water vapour feedback explains 40% of the simulated cooling in all the experiments done.

The transient response of the climate system to both the astronomical and CO_2 forcing was also simulated by the LLN (Louvain-la-Neuve) 2.5-dimensional model over the two last glacial–interglacial cycles. It is particularly significant that spectral analysis of the simulated Northern Hemisphere global ice volume variations reproduces correctly the relative intensity of the peaks at the orbital frequencies. Except for variations with timescales shorter than 5 ka, the simulated long-term variations of total ice volume are comparable to that reconstructed from deep sea cores. For example, the model simulates glacial maxima of similar amplitudes at 134 ka BP and 15 ka BP, followed by abrupt deglaciations. The complete deglaciation of the three main Northern Hemisphere ice sheets, which is simulated around 122 ka BP, is in partial disagreement with reconstructions indicating that the Greenland ice sheet survived during the Eemian interglacial. The continental ice volume variations during the last 122 ka of the 200 ka simulation are, however, not significantly affected by this shortcoming.

1. THE LAST TWO GLACIAL–INTERGLACIAL CYCLES SIMULATED BY THE LLN MODEL

Climate models can be divided into two very broad categories: (i) general circulation models (GCMS); and (ii) statistical-dynamical models, which include energy balance models (EBMS) and two-dimensional zonally averaged dynamical models (Kutzbach 1985). Both GCMS and statistical-dynamical models have been used for the modeling of palaeoclimates. GCMS have been used for simulating geographic features of palaeo-

Phil. Trans. R. Soc. Lond. B (1993) **341,** 253–261
Printed in Great Britain

climates and for including, in the most explicit form, processes such as precipitation that depend on details of the atmospheric flow (Prell & Kutzbach 1987; Rind *et al.* 1989). On the other hand, statistical-dynamical models have a great potential for long-period climate simulations (Berger *et al.* 1990; Deblonde & Peltier 1991*a*,*b*; Gallée *et al.* 1992). As their dimensionality is reduced, they consume less computer time, thus allowing them to take into account all the different parts of the climate system in an interactive and time-dependent way.

Since the publication of the historic Hays *et al.* (1976) paper, a number of modelling efforts have attempted to explain the relation between astronomical forcing and climate change. Most of these modelling studies have focused on the origin of the 100 ka cycle in ice volume. These studies have been motivated by the recognition that the amount of insolation perturbation at 100 ka is not enough to cause a climate change of ice-age magnitude.

It was suggested earlier (Berger 1976, 1979) that the time-evolution of the latitudinal distribution of the seasonal pattern of insolation is the key factor driving the behaviour of the climate system where the complex interactions between its different parts amplify this orbital perturbation. That dynamical behaviour of the seasonal cycle suggests that time-dependent coupled climate models might be able to test whether or not the astronomical forcing can drive the long-term climatic variations.

Such a climate model which links the Northern Hemisphere atmosphere, ocean mixed layer, sea-ice and continents has been validated for the present-day climate (Gallée *et al.* 1991). It is a latitude–altitude model. In each latitudinal belt, the surface is divided into at most five oceanic or continental surface types, each of which interacts separately with the subsurface and the atmosphere. The model explicitely incorporates detailed radiative transfer, surface energy balances, and snow and sea-ice budgets.

This LLN climate model was then asynchronously coupled to a model of the three main Northern Hemisphere ice sheets and their underlying bedrock in order to assess the influence of several factors (processes and feedbacks), including snow surface albedo over the ice sheets, upon ice-age simulations using astronomically derived insolation and CO_2 data from the Vostok ice core (Berger *et al.* 1990; Gallée *et al.* 1992).

The model was first run with ice-sheet feedback by forcing it only with the astronomical insolation over the past 122 ka (Berger 1978) keeping the CO_2 concentration at the Eem level ($\sim$270 p.p.m.v.). Large variations of ice volume are simulated between 122 and 55 ka BP, with a rapid latitudinal extension of the North American and Eurasian ice sheets starting at 120 ka BP. The model simulates a maximum ice volume of 40×10^6 km^3 at roughly 20 ka BP and a total deglaciation as well, this simulation of both the glaciation and deglaciation being a crucial test of the efficiency of the model. The simulated evolution of the three northern ice sheets is generally in phase with geological reconstructions. The major discrepancy between the simulation and observations lies in the temperature variations and in the ice-sheet extent, a discrepancy linked to an overestimation of the CO_2 concentration which was assigned an interglacial value at the last glacial maximum. A final set of experiments therefore addresses the effect of CO_2 on the climate of the last glacial maximum. This experiment made by forcing the model with both insolation and CO_2 variations over the last 122 ka (Barnola *et al.* 1987) significantly improved the temperature results and the ice volume reconstructions obtained in the insolation-only experiment (Gallée *et al.* 1992).

The simulated total ice volume deviation from present day value (assumed to be 30.5×10^6 km^3, that is, 27.9×10^6 km^3 for Antarctica and 2.6×10^6 km^3 for Greenland; Hughes *et al.* 1981) is displayed in figure 1 as a function of time compared to the variation of the global seawater oxygen isotopic ratio given by Labeyrie *et al.* (1987) and Duplessy *et al.* (1988). The latter values are scaled and plotted such that their maximum corresponds to the deviation from present-day of the last glacial maximum total ice volume (taken as 48.6×10^6 km^3; reconstructed by Marsiat & Berger 1990). The simulated deviations are obtained by adding the Northern Hemisphere ice volume changes simulated by the model for each of the individual ice sheets (Eurasia, Greenland, North America) and the changes in Antarctica reconstructed as follows. We assumed: (i) that the Antarctic ice volume at 122 ka BP and from 6 ka BP to the present was the same as now (J. Oerlemans & D. Raynaud, personal communication, 1987); (ii) that 18 ka ago, it was 9.8×10^6 km^3 larger than today (Hughes *et al.* 1981); and (iii) that intermediate values are given by linear interpolation. (Assumption (ii) seems to be in agreement with the recent results obtained by Huybrechts (1990) from a three-dimensional ice sheet model; variation of his Antarctic simulated ice volume between 16 ka BP and to-day, which depends however on sea level variation rather than on precipitation variations, amounts to 7.5×10^6 km^6.)

The main characteristic of figure 1 is the similarity between the reconstructed and the simulated global ice volumes, except for variations with timescales shorter than 5 ka and for an overestimation of the calculated ice volume during isotopic stage 3 when compared to Labeyrie *et al.* (1987). Large ice volume oscillations are found between 122 ka BP and 55 ka BP, while the deglaciation is abrupt both in reconstruction and in simulation. The ice volumes for each ice sheet simulated by the LLN model are also in good agreement with independent reconstructions made from proxy data by Mangerud (1991) and Boulton *et al.* (1985). At 19 ka BP, the simulated temperature of the Northern Hemisphere is 3.4°C colder than the present day simulated value, and the simulated total ice volume deviation is 53×10^6 km^3.

But an obvious experiment (called the 200 ka experiment) to be done with the LLN 2.5-dimensional model was to force it by astronomically driven insolations and by prescribed CO_2 concentrations over the last 200 ka (Gallée *et al.* 1993), in order to confirm the ability of the model to sustain glacial–interglacial

PHILOSOPHICAL TRANSACTIONS OF THE ROYAL SOCIETY B BIOLOGICAL SCIENCES

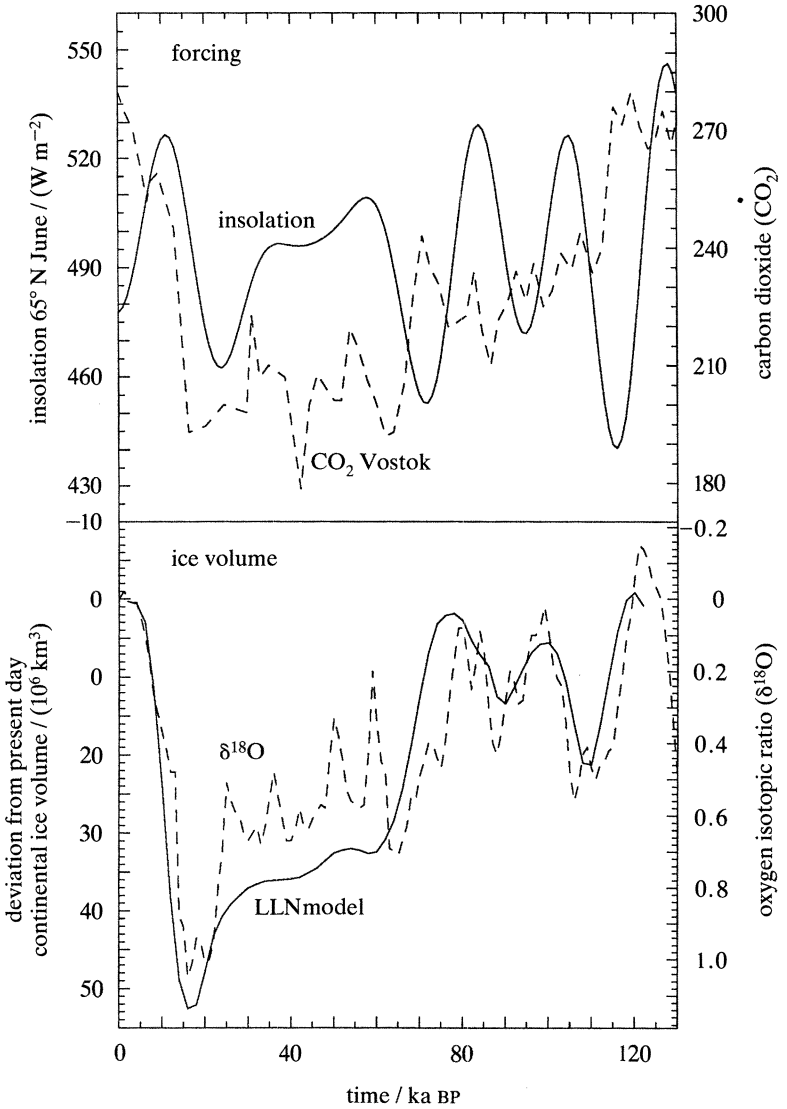

Figure 1. Simulated total ice volume deviation from present-day value assumed to be 30.5×10^6 km^3 (lower panel, full line; Gallée *et al.* 1992). This is compared to the variation of the global sea water oxygen isotopic ratio (lower panel, dashed line) given by Labeyrie *et al.* (1987). These values are scaled and plotted such that their maximum corresponds to the deviation from present-day of the last glacial maximum total ice volume taken as 48.6×10^6 km^3 (Marsiat & Berger 1990). The upper panel provides the long term variations of the June insolation at 65°N (full line; Berger 1978) and of the Vostok CO_2 concentration (dashed line; Barnola *et al.* 1987).

cycles. The Vostok ice core (Barnola *et al.* 1987) does not provide a reconstruction of CO_2 concentration variations before 150 ka BP, so that the model was forced by CO_2 concentrations adapted from Shackleton *et al.* (1992). The simulation starts assuming that the ice sheets are melted at 200 ka BP, because this time corresponds to an interglacial in marine $\delta^{18}O$ records. Two glacial maxima comparable in amplitude are simulated, at 134 and 15 ka BP as found in the marine $\delta^{18}O$ records (e.g. Imbrie *et al.* 1984; see figure 2). The phase lags between the insolation minima at 65°N and ice volume maxima are respectively 6, 5, 6, 11 and 8 ka for the ice volume maxima at 180, 134, 109, 59 and 15 ka BP.

A further comparison of the results of the 200 ka experiment with the SPECMAP record is made in figure 2. The variations correlate well and a spectral analysis of both time series gives spectral peaks of similar amplitude for the 100, 41, 23 and 19 ka periods. The correct relative intensity of the spectral peaks for the simulated ice volume is probably the most important result of this 200 ka experiment as it demonstrates the ability of the LLN model to reproduce the 100 ka cycle. Moreover, the LLN model simulates a deglaciation centred on 130 ka BP and a stable interglacial with high sea-level lasting from about 127 ka BP to 115 ka BP. This duration agrees well with geological evidence for the last interglacial (Müller, 1989), whereas a major weakness both of the SPECMAP record and of previous model simulations (e.g. Imbrie & Imbrie 1980; Berger *et al.* 1981) is precisely their inability to depict the several thousand-year-long stable interglacials.

Finally, an important difference between the atmospheric CO_2 forcing in the 200 ka and 122 ka experiments is observed just before and during isotopic stage

PHILOSOPHICAL TRANSACTIONS OF THE ROYAL SOCIETY B BIOLOGICAL SCIENCES

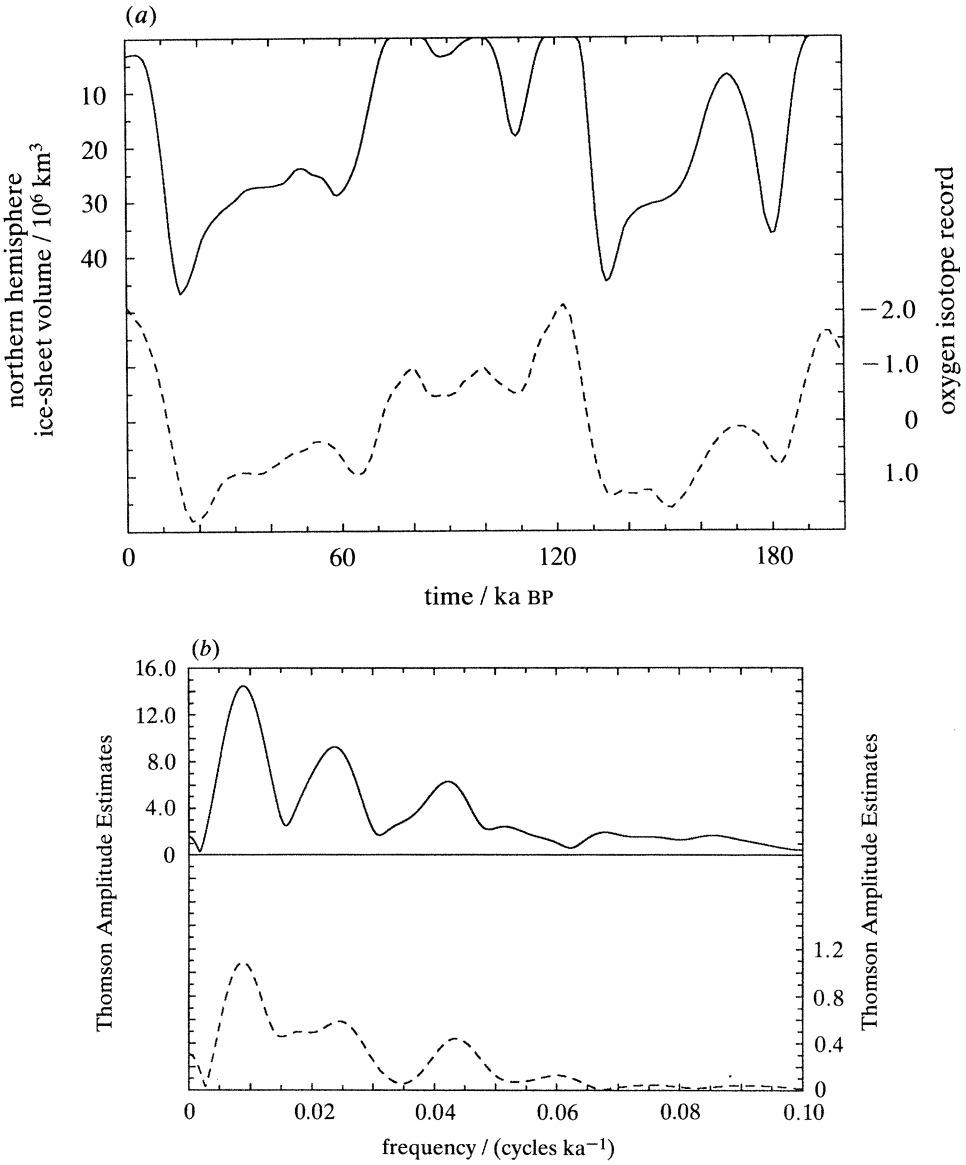

Figure 2. (*a*) Variations over the last 200 ka of: (i) the simulated ice volume of the northern hemisphere (solid curve) (Gallée *et al.* 1993); and (ii) δ^{18}O variation as reconstructed in the SPECMAP time series (short-dashed curve) (Imbrie *et al.* 1984; Martinson *et al.* 1987). The forcing used in the simulation is the insolation variation at the top of the atmosphere and the CO_2 variation adapted from Shackleton *et al.* (1992). (*b*) Spectral amplitude in the Thomson multi-taper harmonic analysis of: (i) the simulated ice volume of the Northern Hemisphere for the 200 ka experiment (solid curve); and (ii) δ^{18}O variation over the last 200 ka as reconstructed in the SPECMAP time series (short-dashed curve).

5e. There is a substantial phase shift between the Barnola *et al.* (1987) and Shackleton *et al.* (1992) reconstructions at this time. In particular, the CO_2 increase (before this interglacial) in the Barnola reconstruction is earlier than Shackleton's reconstruction by 8 ka. More precisely, the maximum in CO_2 concentration occurs at 126 ka BP in the Shackleton *et al.* (1992) data, adopted for the 200 ka experiment, but occurs at 134 ka BP in the Barnola *et al.* (1987) data. In order to assess this impact, a sensitivity experiment has been done by forcing the model with the Barnola *et al.* (1987) CO_2 data and starting at 150 ka BP with the ice sheet configuration as it is simulated in the 200 ka experiment at this time. This experiment is referred to as the 150 ka experiment.

It is remarkable that the CO_2 lag does not significantly affect the time of the ice volume maximum: this maximum occurs at 134 ka BP in the 200 ka experiment and at 136 ka BP in the 150 ka experiment (for comparison, the age given in the SPECMAP chronology (Martinson *et al.* 1987) is 135 ka BP). This suggests that in our model, the timing of the simulated ice volume variations is more tightly locked to the timing of insolation variations than to the timing of CO_2 variations.

At the penultimate glacial maximum, the CO_2 lag impacts more significantly upon the ice volume than its phase. The penultimate ice volume maximum in the 150 ka experiment is lower than that of the 200 ka experiment by 6×10^6 km^3. The 200 ka experiment

gives two glacial maxima of comparable amplitude, a feature which is in agreement with the SPECMAP reconstruction. In the 150 ka experiment the continental ice volume at the last glacial maximum is very similar to that of the 200 ka experiment, and thus of larger amplitude than that of 136 ka BP. Consequently, the difference in the simulated penultimate glacial maximum ice volumes favours the CO_2 chronology proposed by Shackleton *et al.* (1992) and used in the 200 ka experiment, although there is no doubt that as regards actual CO_2 concentration the direct measurements of Barnola *et al.* (1987) are to be preferred.

2. THE FEEDBACK MECHANISMS

One important feature of this LLN model is that it simulates both the glaciation and deglaciation of the last two climatic cycles. This is due to a number of feedbacks introduced in the model. Although these represent only a subset of all the feedbacks acting in the climate system, it is useful to analyse their relative contributions.

(*a*) *Entering the glaciation*

At 60°N, insolation starts to decrease at 133, 127 and 121 ka BP for March, June and September respectively. Summer insolation therefore peaked around 123 ka BP at high northern latitudes. The minimum is reached 11 to 12 ka later. For June, insolation decreases from 545 W m^{-2} to 440 W m^{-2}, a decrease of almost 20%. These latitudes and months are characterized by a strong precession signal whereas in December obliquity dominates the spectrum at this latitude (insolation maxima and minima are alternatively reached at 147, 129, 115 and 88 ka BP).

Each time this type of decrease in insolation occurs, positive feedbacks amplify the response of the climate system to such changes in the external forcing, an amplification which leads to ice sheets accumulating not only up to the time of minimum insolation but continuing to accumulate until a few thousand years later (4–5 ka) due to the inertia of the slow-response part of the system. During these latter periods, negative feedbacks progressively slow the build-up of the ice sheets until they begin to retreat and melt following the ice maximum.

When insolation decreases, surface temperature decreases which delays the melting of snow fields in high latitudes. At the same time, taiga is replaced by tundra which increases the albedo of the vegetated surface covered by snow. Both the snow fields and tundra are therefore leading to an increase of the surface albedo creating a positive feedback. This is reinforced by the subsequent decrease of water vapour content of the atmosphere that results in a decrease in the downward infrared radiation at the surface. But this cooling is also responsible for decreases of the upward infrared, of the latent heat and of the sensible heat fluxes at the surface which feedback negatively on surface temperature.

During this initiation phase, which lasts roughly 4 ka, the zonal mean temperature cooling at the surface leads to a cooling in the atmosphere which, with the insolation decrease, impacts the ice-surface energy budget. The ice-surface temperature does not reach the melting point, even in summer. This means that we have a net accumulation at the surface, ablation being suppressed. As a consequence, the ice sheets are growing which depresses the lithosphere below. With the altitude of the ice sheets increasing, the temperature at their surface decreases (a positive feedback) which progressively decreases the snowfall (a negative feedback) and finally stops the growth of the ice sheet. At the same time, the ice sheets extend to the south. Because of the continentality effect, snowfall at the top of the ice sheets in the interior of the continents decreases (a negative feedback), slowing down the southwards motion of the southern front of the ice sheets. Finally, the maximum volume of ice is reached at 110 ka BP, 4 ka later than the minimum of insolation.

(*b*) *The deglaciation process*

As insolation had already started to increase 4 ka before the ice maximum, this increase starts to be important at 110 ka BP, particularly at the southern edge of the ice sheets which begin to melt. At the same time, the decreased snow fall triggers the 'snow ageing' process which is more efficient in regions of the ice sheets where the temperature is above -10°C. This significantly decreases the albedo of both non-melting and melting snow cover, mainly to the south. In the meantime, snow accumulation has remained positive over the nothern part of the ice sheets creating a north-to-south flux of ice within the ice sheets. At the southern edge, melting is faster than ice flow and isostatic rebound is not fast enough to level up the ice sheet which could prevent future net ablation above. This is not the case north of the ice sheets where isostatic rebound maintains the ice sheets high allowing the north-to-south flux of ice to continue to be efficient. As a consequence, the ice sheet volumes decrease, the heights of the ice sheets decrease, temperature at their surfaces increases which increases the global ablation. This leads to a decrease of the zonal surface albedo and a further replacement of tundra by taiga which feedbacks positively on the albedo decrease, directly and by reducing the albedo of the continental surfaces covered by snow. This leads finally to a minimum of ice volume reached about 5 ka later than the insolation maximum.

3. THE CO_2–WATER VAPOUR–ALBEDO FEEDBACK MECHANISMS AT THE LGM

The comparison of the results obtained from the transient experiment using the Milankovitch and the Milankovitch + CO_2 forcings shows that, at the Last Glacial Maximum (LGM), the long-term CO_2 changes are responsible for roughly 50% of the temperature change and 30% of the ice volume change. In an attempt to understand the role of the temperature–albedo feedback and the importance of the greenhouse

PHILOSOPHICAL TRANSACTIONS OF THE ROYAL SOCIETY B BIOLOGICAL SCIENCES

gases (water vapour and CO_2), several sensitivity experiments have been made (Gallée *et al.* 1992; Tricot 1992; Berger *et al.* 1992).

In particular, the physical processes responsible for the cooling simulated at the LGM under the forcing of both insolation and CO_2 were investigated with a one-dimensional radiative convective (RCM) climate model (Tricot 1992). The main reasons for using a RCM are the number of experiments to be done to isolate the individual contribution of the main processes involved, the potentiality of a RCM for reaching such an objective (Ramanathan & Coakley 1978) and the fact that it requires much less computational power than the 2.5 dimensional model.

A full description of this RCM, its validation and sensitivity tests are given in Tricot (1992) and Berger *et al.* (1993). In particular, when the CO_2 concentration is doubled (from 330 p.p.m.v. to 660 p.p.m.v.), the instantaneous perturbations of the net radiative budget (before the action of feedbacks) are estimated to be 3.72 W m^{-2} at the tropopause and 1 W m^{-2} at the surface. At equilibrium, the temperature increases by 1.8 K at the surface and in the troposphere and decreases in the stratosphere above 16 km. The sensitivity of the RCM to CO_2 change is thus very similar to that calculated in other sensitivity studies using RCMs with the same basic assumptions (e.g. Ramanathan 1981). Without allowing the water vapour feedback to operate, the warming is reduced to 1.2 K.

As the purpose here is to quantify the relative contribution of each of the main climatic feedbacks, some improvements in the LLN model were first made by Tricot (1992) in such a way that the sensitivity of this modified version, designated as LLN1, to changes in trace gas concentrations will be close to the sensitivity of the RCM itself. These improvements concern mainly the radiative part of the model, involving new infrared and solar radiation schemes, and an explicit computation of the stratospheric temperature. Climatological data about cloud and aerosols also have been revised. LLN1 has been validated for the present-day climate. Its sensitivity to a doubling of CO_2 concentration ($\Delta T = 1.97$ K) is similar to the sensitivity of the original version of the LLN model ($\Delta T = 2$ K).

The cooling at the LGM simulated by LLN1 using the surface boundary conditions calculated by the LLN transient simulation, the seasonal cycle of insolation at 18 ka BP and a CO_2 concentration of 194 p.p.m.v. amounts to 4.5 K. This cooling is associated with an increase of the planetary albedo from 31 to 32.6, an increase of the surface albedo from 16.2 to 19.3 and a decrease in the annually – averaged vertically – integrated water vapour concentration from 2.44 to 1.99 g cm^{-2}.

At the LGM, in addition to the insolation and CO_2 concentration variations, the hemispherically averaged changes in the surface albedo and in the vertical distribution of water vapour are available as part of the LLN1 2.5-dimensional model diagnostics. These changes were inserted one by one or in combination into the RCM.

Experiment 1 (table 1) with RCM is related to the present-day climate and leads to a mean temperature of 288.32 K, very close to the 288.36 K obtained from LLN1, the surface albedo being prescribed to its LLN1 value.

In experiment 2, only the surface albedo is changed to its LGM LLN1 value, the CO_2 and water vapour concentration being kept constant to their present-day value. In such a case, if we accept the Milankovitch hypothesis according to which the insolation variations modify the snow and ice covers in the Northern Hemisphere high latitudes, changing only α_s in the RCM is equivalent to looking for the 'natural' cryospheric response of the climatic system to the insolation variations. The simulated cooling of 1.8 K is important and corresponds to a direct radiative forcing of -5.6 W m^{-2} (i.e. the net radiative budget at the tropopause has decreased – less trapping – by 5.6 W m^{-2}).

If we allow the water vapour feedback to amplify this perturbation (experiment 3), the cooling amounts to 3 K which corresponds to a gain factor R of 1.66, R being given by:

$$\Delta T_s = R \Delta T_{s_0}$$

where ΔT_{s_0} is the response of the RCM without any water vapour feedback. The smaller amount of water vapour in this cooler atmosphere leads indeed to a weakening of the greenhouse effect. It combines with the larger planetary albedo induced by the increase of the surface albedo to produce a total cooling 66% larger than without the water vapour feedback. As a consequence, the water vapour induces a positive feedback mainly through its impact on the greenhouse effect and, in a much smaller amount, through an increase in the planetary albedo related to a smaller absorption of the solar radiation in the atmosphere by the water vapour.

If we now decrease the CO_2 concentration from 'present-day' value (330 p.p.m.v.) to the LGM value (194 p.p.m.v.), the climatic response is a cooling of 0.94°C or 1.57°C respectively without (experiment 4) and with (experiment 5) the water vapour feedback. This corresponds to a gain factor of 1.67 very similar to the value obtained in experiment 3 for the albedo increase. This might be a coincidence and it must be tested in more sophisticated models where geographical contrasts do exist. The change of the surface albedo at the LGM (experiment 3) is indeed largely related to the change of the surface cover in middle and high latitudes, whereas the CO_2 concentration change (experiment 5) is a worldwide phenomenon.

The last two experiments combine the changes in the CO_2 concentration and in the surface albedo. When the water vapour feedback is switched off, the cumulative effect of these forcings leads to a total cooling which is the sum of the individual coolings: $-2.74 = -1.8 - 0.94$. This is expected through a linearization of the problem in the absence of the main nonlinearity related to water vapour feedback. Allowing this water-vapour feedback to amplify the direct initial perturbation leads to a total cooling of 4.51 K (experiment 7), very close to the cooling of 4.46 K calculated by the LLN1 model for the LGM boundary

PHILOSOPHICAL TRANSACTIONS OF THE ROYAL SOCIETY B BIOLOGICAL SCIENCES

Table 1. *Sensitivity experiments of a* RCM *to* CO_2, *water vapour and surface albedo (Tricot 1992)*

(T_s is the annually – and hemispherically – averaged temperature at the surface. ΔQ is the initial radiative perturbation at the tropopause (W m^{-2}) after a possible modification of the CO_2 concentration and of the surface albedo α_s from their values in experiment 1. α_{pl} is the planetary albedo. [H_2O] is the water vapour concentration in (g cm^{-2}). ΔT_{s_0} is the response of RCM without H_2O feedback. f_{H_2O} and R are respectively the feedback factor for H_2O and the gain factor with

$$\Delta T_s = \frac{1}{1-f}\,\Delta T_{s_0} = R\Delta T_{s_0}.)$$

experiments with RCM	T_s K	ΔQ (W m^{-2})	α_{pl}(%)	[H_2O] (g cm^{-2})	ΔT_{s_0} K	ΔT_s K	R
1 present-day climate CO_2 = 330 p.p.m.v. α_s = 16.24 H_2O computed by RCM	288.32		32.85	2.29			
2 CO_2 = 330 p.p.m.v. α_s = 19.25 H_2O fixed as in 1	286.52	−5.62	34.43	2.29	−1.8	−1.8	1.00
3 CO_3 = 330 p.p.m.v. α_s = 19.25 H_2O computed by RCM	285.33	−5.62	34.66	1.88	−1.8	−2.99	1.66
4 CO_2 = 194 p.p.m.v. α_s = 16.24 H_2O fixed as in 1	287.38	−2.91	32.85	2.29	−0.94	−0.94	1.00
5 CO_2 = 194 p.p.m.v. α_s = 16.24 H_2O computed by RCM	286.75	−2.91	32.97	2.07	−0.94	−1.57	1.67
6 CO_2 = 194 p.p.m.v. α_s = 19.25 H_2O fixed as in 1	285.58	−8.53	34.42	2.29	−2.74	−2.74	1.00
7 CO_2 = 194 p.p.m.v. α_s = 19.25 H_2O computed by RCM	283.81	−8.53	34.77	1.70	−2.74	−4.51	1.65

conditions. Even in this case, this total response is more or less the sum of the individual responses (experiments 3 and 5): $-4.51 \simeq -2.99 - 1.57$ because the perturbations are small in amplitude compared to the fundamental state (a few degrees against 288 K). Table 1 thus illustrates the linear theory of feedbacks when the external forcings are due to albedo and CO_2 changes, the only feedback being related in our study to the water vapour concentration change.

In terms of the feedback parameter, λ, used in the theory of the greenhouse effect intensification, we have

$$\Delta T_{s_{equilibrium}} = \Delta Q/\lambda = \Delta T_{s_0}/(1-f) = R\Delta T_{s_0}$$

The feedback factor, $f = 1 - 1/R$, for the water vapour is estimated from experiments 3, 5 and 7 to be roughly $0.4 \cdot \lambda$ in experiments 2, 4 and 6 is equal to 3.1 and in experiments 3, 5 and 7 it amounts to roughly 1.9; this leads to a positive feedback of the water vapour equal to 1.2, a value close to the value (1.4) obtained in the greenhouse theory (e.g. Berger & Tricot 1992). It happens therefore that the water vapour feedback intensity is about independent of the specific character of the prescribed changes.

All these sensitivity tests done with a RCM using the value of the parameters simulated at the last glacial maximum by the LLN1 2.5-dimensional model lead to the following conclusions for the Northern Hemisphere.

1. The cooling using only the astronomical forcing – but allowing for the water vapour feedback – amounts to 3°C, 67% of the 4.5°C cooling resulting from both the astronomical and CO_2 forcings. It must be stressed that what we call astronomical forcing includes both the change in insolation and the consequent changes in surface and planetary albedo.
2. If the CO_2 concentration is kept fixed to its interglacial level (330 p.p.m.v.), the astronomical-albedo forcing without the water vapour feedback (WVF) explains 60% of the 3°C cooling, the water

PHILOSOPHICAL TRANSACTIONS OF THE ROYAL SOCIETY B BIOLOGICAL SCIENCES

vapour feedback being therefore responsible for 40% of the total cooling in this Milankovitch alone experiment.

3. In the astronomical + CO_2 experiment, the direct effect of these forcings (i.e. without the WVF) explains 60% (2.7°C) of the 4.5°C cooling. As in paragraph 2 above, the WVF is therefore responsible for 40% of the cooling. If we discriminate between the astronomical-albedo forcing (AA) and the CO_2 contribution (CO_2), we can see that without the WVF, AA explains 40 of the 60% of the total cooling. The contributions to the WVF (40% of the total cooling) are 27% for AA and 13% for CO_2.
4. In this astronomical + CO_2 cooling, it may also be interesting to analyse the proportion which is due to water vapor for each sub-experiment. Considering only the astronomical–albedo forcing, the WVF is responsible for 27 of the 67% of the global cooling, the remaining 40% is the direct effect of AA. In the CO_2 alone experiment, the WVF explains 13 of the 33% of the global cooling, the direct effect of CO_2 accounting for the remaining 20%.

In summary, the general conclusions are as follows.

1. If we discriminate between the astronomical–albedo forcing and the CO_2 forcing, AA is responsible for 67% and CO_2 for 33% of the cooling, whatever experiment is considered: without WVF, $-2.7 = -1.8 - 0.9$; with WVF, $-4.5 = -3.0 - 1.5$; due to WVF, $-1.8 = -1.2 - 0.6$.
2. If we discriminate between the direct effect of the astronomical-albedo and/or CO_2 forcings and the water vapour feedback contribution, AA and/or CO_2 accounts for 60% and the WVF for 40% of the cooling, whatever experiment is considered: without CO_2, $-3.0 = -1.8 - 1.2$; with CO_2, $-4.5 = -2.7 - 1.8$; due to CO_2 alone, $-1.5 = -0.9 - 0.6$.

4. CONCLUSIONS

Simulation of the advances and retreats of the ice sheets over the last two glacial–interglacial cycles indicates that the orbital parameter variations are able to trigger feedbacks in the LLN model which then induce significant climatic variations at that timescale. We would argue that: (i) because the LLN model reproduces correctly the power spectrum of the reconstructed climatic variations over the last two glacial-interglacial cycles; (ii) because it gives a more realistic depiction of the Eemian interglacial (isotopic stage 5e) and of its length than previous models; and (iii) because its sensitivity to the CO_2 forcing and to the water vapour feedback is similar to that of the more complex GCMs, it is its chronology rather than the SPECMAP chronology that should be the target for testing new radiometric dating methods.

It must be pointed out that the physical processes included in the LLN model are probably not the only ones to play a significant role in the climate system and this simulation must be regarded first of all as an exercise to learn how the coupling of the different components of the climate system works at the astronomical timescale, and to test parameterizations which have appeared in the literature for each individual subsystem. Given that the model has many parameters connected to the numerous processes that are parameterized within it, the fact that it fits more or less one set of data (the present-day climate, for example) is not a definitive test of its physical validity. The most significant result is, however, that among the large number of possible combinations of parameter values allowing a good representation of the present-day climate, only a very limited set allows at the same time reasonable palaeoclimatic reconstruction at the astronomical timescale. It seems unlikely therefore that, by chance alone, such a nonlinear numerical model can simulate the present-day latitudinal and seasonal cycles of many climate variables (Gallée *et al.* 1991) and, simultaneously, slight changes over the last few centuries (Smits *et al.* 1993), changes as large as those projected for the next few decades (Fichefet *et al.* 1989), and the gross features of the low frequency part of the last two glacial–interglacial cycles (Gallée *et al.* 1992, 1993).

In view of the relatively good simulations obtained by the LLN model, there are many important implications that need to be explored. First, were the results fortuitous, or rather, were most of the important processes captured in two dimensions by neglecting such factors as changes in deep water formation? Second, in view of the critical importance of snow–albedo–temperature–vegetation feedbacks on the ice-sheet initiation and deglaciation processes, can the parameterizations of these feedbacks be improved? Third, looking to the sensitivity of all the models used to test the astronomical theory, how are we to distinguish which, if either, of the mechanisms are correct? It would appear that the only acceptable way is to describe more of the physics, chemistry and biology explicitly.

H. Gallée is supported by the Belgian Scientific Research Programme on Antarctica of the Prime Minister's Science Policy Office, and M. F. Loutre is supported by Contract CEA BC-4561 of the Commissariat Français à l'Energie Atomique. This research was sponsored partly by the Climate Programme of the Commission of the European Communities under Grants EV4C-0052-B (GDF) and EPOC-0004 (EDB). Computations with the palaeoclimate model were done using an IBM RS/6000-550 workstation under a study contract between IBM Belgium and the Catholic University of Louvain in Louvain-la-Neuve (1992–1994).

REFERENCES

Barnola, J.-M., Raynaud, Y., Korotkevich, Y.S. & Lorius, Cl. 1987 Vostok ice core provides 160,000-yr record of atmospheric CO_2. *Nature, Lond.* **329**, 408–414.

Berger, A. 1976 Long-term variations of daily and monthly insolation during the last Ice Age. *EOS* **57** (4), 254.

Berger, A. 1979 Insolation signatures of Quaternary climatic changes. *Il Nuovo Cimento*, **2C** (1), 63–87.

Berger, A., Guiot, J., Kukla, G. & Pestiaux, P. 1981 Long term variations of monthly insolation as related to climate change. *Geologischen Rundschau*, Bd. **70** (2), 748–758.

Berger, A., Gallée, H., Fichefet, Th., Marsiat, I. & Tricot, C. 1990 Testing the astronomical theory with a coupled

PHILOSOPHICAL TRANSACTIONS OF THE ROYAL SOCIETY B BIOLOGICAL SCIENCES

climate-ice sheet model. In *Geochemical variability in the oceans, ice and sediments* (ed. L. D. Labeyrie and C. Jeandel) (*Palaeogeogr. Palaeoclim. Palaeoecol.* **89**), pp. 125–141.

Berger, A. & Loutre, M.F. 1991 Insolation values for the climate of the last 10 million years. *Quat. Sci. Rev.* **10**, 297–317.

Berger, A. & Tricot, C. 1992 The greenhouse effect. *Surv. Geophys.* **13**, 523–549.

Berger, A., Gallée, H. & Tricot, C. 1992 Glaciation and deglaciation mechanisms in a coupled 2-D climate – ice sheet model. *J. Glaciol.* (In the press.)

Berger, A., Tricot, C., Gallée, H., Fichefet, Th. & Loutre, M.F. 1993 The last glacial-interglacial cycles with the LLN model. In *NATO ASI on long-term climatic variations—data and modeling*, Siena, Italy (ed. J. Cl. Duplessy). Berlin: Springer Verlag.

Boulton, G.S., Smith, G.D., Jones, A.S. & Newsome, J. 1985 Glacial geology and glaciology of the last mid-latitude ice sheets. *J. geol. Soc. Lond.* **142**, 447–474.

Deblonde, G. & Peltier, W.R. 1991*a* Simulations of continental ice sheet growth over the last glacial-interglacial cycle: experiments with a one level seasonal energy balance model including realistic geography. *J. Geophys. Res.* **96**, 9189–9215.

Deblonde, G. & Peltier, W.R. 1991*b* A one-dimensional model of continental ice volume fluctuations through the Pleistocene: implications for the origin of the Mid-Pleistocene climate transition. *J. Climate* **4** (3), 318–344.

Duplessy, J.Cl., Labeyrie, L. & Blanc, P.L. 1988 Norwegian sea deep water variations over the last climatic cycle: paleo-oceanographical implications. In: *Lond and short term variability of climate* (ed. H. Wanner & U. Siegenthaler), pp. 83–116. New York: Springer-Verlag.

Ellingson, R.G. & Fouquart, Y. 1991 The intercomparison of radiation codes in climate models: an overview. *J. geophys. Res.* **96** (D5), 8925–8927.

Fichefet, Th., Tricot, C., Berger, A., Gallée, H. & Marsiat, I. 1989 Climate studies with a coupled atmosphere-upper ocean-ice sheets model. *Phil. Trans. R. Soc. Lond.* A **329**, 249–261.

Gallée, H., van Ypersele, J.P., Fichefet, Th., Tricot, C. & Berger, A. 1991 Simulation of the last glacial cycle by a coupled sectorially averaged climate – ice-sheet model. I. The climate model. *J. geophys. Res.* **96**, 13139–13161.

Gallée, H., van Ypersele, J.P., Fichefet, Th., Marsiat, I., Tricot, C. & Berger, A. 1992 Simulation of the last glacial cycle by a coupled, sectorially averaged climate – ice-sheet model. II. Response to insolation and CO_2 variation. *J. geophys. Res.* **97** (D14), 15713–15740.

Gallée, H., Berger, A. & Shackleton, N.J. 1993 Simulation of the climate of the last 200 kyr with the LLN 2D-model. In *Ice in the climate system* (ed. R. Peltier). Proceedings of the NATO Advanced Research Workshop, Aussois, France, September 7–11, 1992. (In the press.)

Hays, J.D., Imbrie, J. & Shackleton, N.J. 1976 Variations in the earth's orbit: pacemaker of the ice ages. *Science, Wash.* **194**, 1121–1132.

Hughes, T.J., Denton, G.H., Anderson, B.G., Schilling, D.H., Fasthook, J.L. & Lingle, C.S. 1981 The last great ice sheets: a global view. In *The last great ice sheets* (ed. G. H. Denton & T. J. Hughes), pp. 275–317. Wiley Interscience Publ.

Huybrechts, Ph. 1990 The Antarctic ice sheet during the last glacial-interglacial cycle: a 3-D model experiment. *Ann. Glaciol.* **14**, 115–119.

Imbrie, J. & Imbrie, J.Z. 1980 Modeling the climatic response to orbital variations. *Science, Wash.* **207**, 943–953.

Imbrie, J., Hays, J.D., Martinson, D.G., McIntyre, A., Mix, A.C., Morley, J.J., Pisias, N.G., Prell, W.L. & Shackleton, N.J. 1984 The orbital theory of Pleistocene climate: support from a revised chronology of the marine $\delta^{18}O$ record. In *Milankovitch and climate* (ed. A. Berger *et al.*), pp. 269–305. Dordrecht, Holland: D. Reidel.

Kutzbach, J.E. 1985 Modeling of paleoclimates. *Adv. Geophys.* **28A**, 159–196.

Labeyrie, L.D., Duplessy, J.Cl. & Blanc, P.L. 1987 Variations in mode of formation and temperature of oceanic deep waters over the past 125,000 years. *Nature, Lond.* **327**, 477–482.

Mangerud, J. 1991 The last glacial history of Scandinavia between the last interglacial and the last glacial maximum. In *Klimageschichtliche Probleme der Letzten 130,000 Jahre* (ed. B. Frenzel), pp. 307–330. Akademie der Wissenschaften und der Literatur, Mainz. Stuttgart, New York: Fisher Verlag.

Marsiat, I. & Berger, A. 1990 On the relationship between ice volume and sea level over the last glacial cycle. *Climate Dyn.* **4**, 81–84.

Martinson, D.G., Pisias, N.G., Hays, J.D., Imbrie, J., Moore, T.C. & Shackleton, N.J. 1987 Age dating and the orbital theory of the ice ages: development of a high-resolution 0 to 300,000-year stratigraphy. *Quat. Res.* **27**, 1–27.

McClatchey, R.A., Fenn, R.W., Selby, J.E.A., Volz, F.E. & Garing, J.S. 1972 Optical properties of the atmospheres. *Rep. AFCRL-72-0497*, 3rd edn. (108 pages.) Environmental Research Paper 411, Air Force Cambridge Research Laboratory, Massachusetts.

Müller, H. 1989 Palynologische Untersuchung eemzeitlicher Ablagerungen einer 15 km westlich Sylt niedergebrachten Kernbohrung. *Probleme der Küstenforschung im südlichen Nordseegebiet* **17**, 119–124.

Oort, A.H. 1983 Global atmospheric circulation statistics 1958–1973. *NOAA professional paper 14.* (180 pages.)

Prell, W.L. & Kutzbach, J.E. 1987 Monsoon variability over the past 150,000 years. *J. geophys. Res.* **92**, 8411–8425.

Ramanathan, V. 1981 The role of ocean-atmosphere interactions in the CO_2 climate problem. *J. Atmos. Sci.* **38**, 918–930.

Ramanathan, V. & Coakley, J.A. Jr 1978 Climate modeling through radiative convective models. *Rev. Geophys. Space Phys.* **16**, 465–489.

Ramanathan, V. & Dickinson, R.E. 1979 The role of stratospheric ozone in the zonal and seasonal radiative energy balance of the Earth troposphere system. *J. Atmos. Sci.* **36**, 1084–1104.

Rind, D., Peteet, D. & Kukla, G. 1989 Can Milankovitch orbital variations initiate the growth of ice sheets in a general circulation model? *J. geophys. Res.* **94** (D10), 12851–12871.

Schneider, S.H. & Thompson, S.L. 1979 Ice ages and orbital variations: some simple theory and modelling. *Quat. Res.* **12**, pp. 188–203.

Shackleton, N.J., Le, J., Mix, A. & Hall, M.A. 1992 Carbon isotope records from Pacific surface waters and atmospheric carbon dioxide. *Quat. Sci. Rev.* **11**, 387–400.

Smits, I., Fichefet, Th, Tricot, C. & van Ypersele, J.P. 1993 A model study of the time evolution of climate at the secular time scale. *Atmosfera.* (In the press.)

Tricot, C. 1992 Sur la contribution des gaz à effet de serre dans les changements climatiques à long terme. Thèse de doctorat, Faculté des Sciences, Université Catholique de Louvain.

PHILOSOPHICAL TRANSACTIONS OF THE ROYAL SOCIETY B BIOLOGICAL SCIENCES